SOCIAL SCIENCES: Psychological and Cognitive Sciences

Revisiting the Neural Architecture of Decision-Making: Univariate and Multivariate Evidence for System-Based Models in Adolescence

João F. Guassi Moreira*, Adriana S. Méndez Leal, Yael H. Waizman, Natalie Saragosa-Harris, Emilia Ninova, & Jennifer A. Silvers*

Department of Psychology, University of California, Los Angeles

***corresponding authors**
A191 Franz Hall
502 Portola Plaza
Los Angeles CA, 90095-1563
jguassimoreira@ucla.edu
silvers@ucla.edu

Author Contributions
J.F. Guassi Moreira and J.A. Silvers developed and designed research questions and study concept. Data were collected by J.F. Guassi Moreira, A.S. Méndez Leal, Y.H. Waizman, N. Saragosa-Harris, E. Ninova. Data were prepared and analyzed J.F. Guassi Moreira under the supervision of J.A. Silvers with feedback from A.S. Méndez Leal, Y.H. Waizman, N. Saragosa-Harris, and E. Ninova. J.F. Guassi Moreira drafted the first version of the manuscript with critical input from J.A. Silvers. All authors provided critical revisions and approved the final manuscript for submission.

Competing Interest Statement
None

This file includes:
Main Text
Figures 1 to 3
Tables 1 to 2
Supplementary Materials

Word Count: 7046
Reference Count: 71

Abstract

System-based theories are a popular approach to explaining the psychology of human decision making. Such theories posit that decision-making is governed by interactions between different psychological processes that arbitrate amongst each other for control over behavior. To date, system-based theories have received inconsistent support at the neural level, leading some to question their veracity. Here we examine the possibility that prior attempts to evaluate system-based theories have been limited by their reliance on predicting brain activity from behavior, and seek to advance evaluations of system-based models through modeling approaches that predict behavior from brain activity. Using within-subject decision-level modeling of fMRI data from a risk-taking task in a sample of over 2000 decisions across 51 adolescents—a population in which decision-making processes are particularly dynamic and consequential—we find support for system-based theories of decision-making. In particular, neural activity in lateral prefrontal cortex and a multivariate pattern of cognitive control both predicted a reduced likelihood of making a risky decision, whereas increased activity in the ventral striatum—a region typically associated with valuation processes—predicted a greater likelihood of engaging in risk-taking. These results comprise the first formalized within-subjects neuroimaging test of system-based theories, garnering support for the notion that competing systems drive decision behaviors.

Significance Statement

Decision making is central to adaptive behavior. While dominant psychological theories of decision-making behavior have found empirical support, their neuroscientific implementations have received inconsistent support. This may in part be due to statistical approaches employed by prior neuroimaging studies of system-based theories. Here we use brain modeling—an approach that predicts behavior from brain activity—of univariate and multivariate neural activity metrics to better understand how neural components of psychological systems guide decision behavior. We found broad support for system-based theories such that that neural systems involved in cognitive control predicted a reduced likelihood to make risky decisions, whereas value-based systems predicted greater risk-taking propensity.

Introduction

Effective decision-making is central to adaptive behavior and is thus unsurprisingly one of the most widely studied phenomena in behavioral science. From Ancient Greek philosophers to present day neuroscientists, human history has no shortage of theoretical perspectives on what drives and explains human decision-making (1). In psychology, some of the most heavily cited and intuitive of these theories are system-based, whether they aim to directly explain decision-making behavior or its causal antecedents (e.g., self-control (2)). Both classic and modern system-based theories posit that decision-making is governed by psychological processes that compete (or in some cases, complement) to guide behavior (2–5). Such system-based theories have been applied to adolescent risk-taking (3,6,7), self-control (2), moral decision-making (8,9), and financial behavior (10). Despite their broad success at describing the psychological underpinnings of decision behavior, these theories have yielded mixed support when adapted to describe the underlying neurobiology of decision-making (e.g., 11). This discrepancy between psychological and neural evidence for system-based theories may be due to the facts that most prior neuroimaging work on this topic has employed brain mapping (predicting brain from behavior) instead of brain modeling (predicting behavior from brain) approaches, tested theory at between- instead of within-subject levels, and did not consider the role of multivariate neural patterns. The current study sought to address these methodological limitations in a neuroimaging study of adolescent risky decision-making. Adolescents are the ideal population for this research because (i) brain systems underlying decision-making and associated processes (e.g., self-control) develop dramatically in adolescence (2,12,13); (ii) system-based accounts have had an outsized influence on conceptualizations of adolescent neurodevelopment and behavior (3,6); (iii) system-based theories in this domain routinely find strong support at the psychological level but inconsistent support at the neural level (14); (iv) this topic has important implications for public health and judicial policy given that numerous risky behaviors peak during adolescence (15,16).

A number of system-based theories have been used—directly or indirectly—to explain risky decision making and other motivated behaviors in adolescence (2,12,17–19). Most of these theories posit the existence of two (though some posit three or more) adversarial systems: A value-based system which is oriented toward immediate incentives, is thought to increase propensity for risk-taking; whereas a cognitive control system is purportedly tasked with restraining the former system and avoiding risks. Prominent theories have argued that during adolescence, the value-based system is primed to ‘overpower’ the cognitive-control system, ostensibly leading adolescents to take more risks than children and adults – particularly in socioemotional contexts (3,20).

System-based models tend to perform well at explaining adolescent behavior across a variety of methodologies (20–23). For example, cross-sectional age-related differences in cognitive control and reward sensitivity map onto adolescent-specific increases in risky behavior

(24). Consistent evidence has also been observed in lab contexts, where experimental manipulations of the value-based system have been shown to interfere with cognitive control performance, especially in adolescents (21). By contrast, *neuroscientific evidence* for these theories has been far less consistent (25–30). These inconsistencies have prompted some to advocate for updating simple system-based models with circuit-based (2) or whole-brain network accounts of adolescent neurodevelopment (31). Others have suggested that system-based theories are biologically implausible and ought to be dismissed altogether (11,32). Without rejecting these possibilities, we propose an alternative interpretation for why system-based theories may receive inconsistent neuroscientific support. We argue that these inconsistences in neuroscientific findings might be addressed through philosophical and methodological adjustments that may facilitate replication and theory validation.

Prior neuroscientific investigations of system-based theories, in adolescence as well as in other developmental periods, have relied heavily on univariate *brain mapping* methods. Brain mapping refers to the process of attempting to statistically predict brain activity either from stimulus characteristics or from behavior on a task that ostensibly indexes a psychological process of interest (33). For example, in the context of decision making one might compare neural activation associated with risky decisions to neural activation associated with safe decisions. An alternative to brain mapping is brain modeling (33), which seeks to use neuroscientific data to predict cognitions and behavior, rather than the other way around (i.e., using brain activity to predict when one is likely to make a risky or safe decision). While brain mapping has led to a number of key discoveries in cognitive neuroscience (e.g., Kanwisher, 2017), it can be problematic for the purposes of evaluating system-based theories. This is because system-based theories seek to make predictions about how underlying processes – for example, "when brain activity related to cognitive control is high, individuals will be less likely to take a risk" – which almost by definition aligns itself to a brain modeling approach, as it explicitly assumes behavior is the result of neural computations (e.g., task behavior = *f*(brain)). Brain modeling has been argued to be more optimal than brain mapping because individual units of analysis (e.g., voxels, neurons, etc.) are more predictive when used in concert (such as in a multivariate signature) to predict task behavior, as opposed to the opposite (task features predicting brain) (33,35).

Another potential limitation of prior neurodevelopmental studies of risky decision-making is that most have focused on between-subject differences in risk taking behavior, rather than within-individual differences (22,23,25–28,36). However, most prior work has examined between-subject dynamics and the role of external factors in shaping behavior (e.g., peer or adult present during decision-making; affective versus neutral stimuli (37,38)). While useful, the focus on these issues means that the core, fundamental tenets of system-based theories (i.e., brain systems predict dynamic changes in behavior) remained untested. This omission is somewhat surprising given that most system-based theories of decision-making are implicitly geared

towards explaining within-subject behavior (2,17). A second issue is that system-based theories are almost exclusively expressed in linguistic, rather than numeric, terms (39). In other words, system-based theories have not been articulated mathematically, rendering it difficult to determine whether study results support or contradict systems-based theories.

The current study is to the best of our knowledge, the first within-subject, brain modeling investigation of system-based theories of adolescent decision-making. Using functional magnetic resonance imaging (fMRI), we predicted trial-by-trial risky decision-making in healthy adolescents as a function of brain activity from value-based and cognitive control systems, as posited by system-based models. Critically, we examined two versions of value-based and cognitive control systems: a 'classic' version and a newly posited 'switchboard' version. The classic variant of the theory assumes that the value-based system that prioritizes immediate rewards is primarily housed in the nucleus accumbens (NAcc) whereas the cognitive control system is located in lateral prefrontal cortex (lPFC) (3). This variant is clearly modular, in that it posits that psychological functions are represented in isolated brain regions, or modules, that independently and locally perform their respective function. While evidence exists to suggest that some degree of modularity may be present in the brain (34), this assumption is inconsistent with much other work in cognitive neuroscience that shows psychological processes are encoded in distributed, multivariate signatures (40,41). To that end, we additionally tested a 'switchboard' version of the model wherein we predict risky behavior as a function of multivariate neural signatures of value and cognitive control (via the use of multivoxel pattern analysis; MVPA). The advantage of this approach is that it does not hypothesize the localization of mental function to any given ROI—it instead assumes that mental functions are encoded in distributed patterns, which is consistent with recent advances in cognitive neuroscience (42). Another way to summarize the two variants of the model is that the functional units of the classic model lie in particular ROIs, whereas the functional units of the switchboard model are comprised by patterns of activity that cut across brain regions. We used multilevel logistic regression to examine how linear combinations of these brain metrics predicted *within-person* risky behavior. Last, for thoroughness we also implemented a between-subjects version of the model (predicting risky behavior as a function of brain metrics using only between-subjects information).

Methods

Procedures and Measures

Participants. The 51 participants (Mean age = 15.00 years, SD = 3.66, range = 9.11 - 22.60[1], 25 females) in the current study were part of a broader longitudinal study investigating the impact of early life experiences on the neural bases of socioemotional development. Participants in the current set of analyses were those who provided usable data from an fMRI scanning session and did not have a history of early social deprivation. Ethnically, eight

[1] This age range is consistent with recent scientific advances that suggest adolescence in human development may last nearly fifteen years (71)

participants identified as Hispanic/Latinx (15.7%). Racially, twenty-six participants identified as white (51%), six participants (11.8%) identified as Asian/Asian American, one participant (2%) identified as Native Hawaiian/Other Pacific Islander, seven participants (13.7%) identified as African American, no participants (0%) identified as Native American/Alaskan Native, four participants (7.8%) identified as being mixed race, four participants identified as belonging to an unlisted race (7.8%), and three participants (5.9%) declined to report their race. Sample size was dictated by the number of participants willing to participate in this wave of data collection. Participants were compensated $50 (USD) for participating in fMRI scanning. The research was completed at the University of California, Los Angeles (UCLA). All participants under 18 years provided informed assent and their parents provided informed consent; all participants 18+ years provided informed consent. All research practices were approved by the Institutional Review Board at the University of California, Los Angeles. Data and analysis code are publicly available on the Open Science Framework (OSF; osfi.io/fphn4).

Risk-Taking Paradigm. Participants completed the Yellow Light Game (YLG) while undergoing fMRI scanning (Figure 1A; 43). An adaptation of a widely used adolescent risk-taking task (the stoplight game; 44–46), the YLG is a computerized driving simulation in which participants drive along a straight road and encounter a series of intersections. Consistent with prior studies, participants in our study were told the objective of the game was to drive through the set of intersections as quickly as possible. The traffic light at each intersection turned yellow for 1000ms prior to crossing each intersection and participants were faced with a choice to brake ('stop') or drive through the intersection ('go'). A choice to brake at the intersection resulted in a delay of 2500ms. A choice to accelerate through the intersection resulted in one of two outcomes -- (i) participants would drive straight through the intersection with no delay, or (ii) a car from the cross-street would crash into them resulting in a 5000ms delay. A 10000ms delay was imposed if participants failed to respond on a trial. Participants made their choices by pressing one of two buttons on a button box using their index and middle fingers.

Participants completed three runs of the task, consisting of 15 trials each. Unbeknownst to participants, five intersections per run were set to result in a crash if participants chose to accelerate through them, meaning that the probability of crashing was equal to ⅓. Participants were not made aware of this probability. Each run had specific intersections that were rigged to crash and the order in which runs were administered was counterbalanced across participants. Buttons indicating 'go' and 'stop' were also counterbalanced between subjects amongst the index and middle fingers. The task was self-paced but typically took participants approximately 2.5 minutes to complete each run. Participants completed two, 10-trial practice runs prior to scanning in order to eliminate any potential confounds associated with learning. The YLG was programmed in Java and ran off Apache Tomcat, a program that creates a HTTP web-server environment.

fMRI Data Acquisition. Imaging data were acquired on a 3T Siemens Prisma scanner using a 32-channel head coil and a parallel image acquisition system (GRAPPA). A high resolution T1-weighted, magnetization-prepared rapid acquisition gradient echo (MPRAGE) image was acquired for registration to functional runs (TR = 2400ms, TE = 2.22ms, flip angle = 8°, FoV = 256mm^2, 0.8mm^3 isotropic voxels, 208 slices). Functional images were acquired using a T2* EPI BOLD sequence. Thirty-three axial slices were collected with a TR of 2000ms and a 3 x 3 x 4 mm^3 voxel resolution (TE = 30ms, flip angle = 75°, FoV = 192mm^2). Participants completed the YLG by using a head-mounted on the coil to view an LCD back projector screen.

fMRI Analysis

The following sections describe our approach to analyzing the fMRI data using both univariate activity estimates of the NAcc and lPFC and multivariate pattern expression values for reward and cognitive control signatures (signature definitions described below). We first describe our preprocessing steps and then outline the single trial analysis procedure used to produce both univariate activity estimates and multivariate metrics for each trial during the task. Because we were interested in within-subject variability in decision making, we estimated univariate and multivariate values for each trial across all subjects. Single-trial metrics were used for both the within-person (in disaggregate form) and between-person (in aggregate form) analyses, for consistency.

Preprocessing

Prior to preprocessing, functional images were visually inspected for artifacts and biological abnormalities. No images contained obvious artifacts or biological abnormalities that warranted exclusion from further analysis. fMRI data were preprocessed and analyzed using the fMRI Expert Analysis Tool (FEAT, version 6.00) of the FMRIB Software Library package (FSL, version 5.0.9; fsl.fmrib.ox.ac.uk). Preprocessing consisted of the following steps: We used the brain extraction tool (BET) to remove non-brain tissue from functional and structural runs, spatially realigned functional volumes to the middle image to correct for head motion using MCFLIRT, and high-pass filtered the data with a 100-s cutoff. We used fsl_motion_outliers to identify volumes that exceeded a 0.9mm frame displacement (FD) threshold for head motion (Siegel et al., 2014), though most participants failed to record any volumes exceeding this threshold (Supplementary Table 1; Supplementary Figure 1). No participant had more than 10% of their volumes in a given run exceed the aforementioned framewise displacement threshold and thus, no participants were excluded on the basis of head motion in our sample. Spatial smoothing was not conducted during preprocessing and was instead applied later when extracting data from single trial activity estimates because the extent of smoothing depended on the type of information that was being extracted from the single trial (average ROI activation warrants greater smoothing than pattern expression analysis). We prewhitened the data to correct for autocorrelated residuals across time. Functional data were registered to each subject's high resolution MPRAGE scan with FSL's boundary-based registration (47) while maintaining the 3 x

3 x 4 mm voxel size. To preserve the fine-grained spatial resolution of the data, we did not register the functional runs to standard MNI space at this stage but did so for the traditional group analyses reported in the Supplement. As detailed below, masks and neural signatures were defined in standard space and then transformed to subject space.

Within-Subject Analyses.

Single Trial Activity Estimation. We used a least squares analytic framework to obtain trial-level estimates of the BOLD signal (i.e., a beta-series; 48). Here we opted to use the least squares single (LSS; Figure 1B) method, due to its advantageous statistical properties over the least squares all (LSA) estimator, especially considering the fast timing of the YLG (49,50). Accordingly, a fixed-effects General Linear Model (GLM) was created for the decision period on each trial of the YLG game within each participant. A decision period was defined as the time between the onset of the yellow light (i.e., when the light at the traffic intersection switched to yellow from green as the car approached the intersection) and when participants pressed a button to signify their decision. A GLM was modeled for the *i*-th decision period (target decision) such that the target decision received its own regressor, all other decision periods were modeled in a single, separate nuisance regressor, and outcomes of all decisions (delays due to the braking, successful passes after running the light, or crashes) were modeled in another regressor.

Head motion was statistically controlled for across all GLMs by adding FSL's extended motion parameters (6 regressors for x, y, z, pitch, roll, yaw directions, their squares, and their derivatives, comprising 24 regressors) in addition to regressors for single volumes that exceeded a frame displacement threshold of 0.9mm (i.e., censoring). The first temporal derivative of all task and motion regressors were also entered into the model in order to account for any slice timing effects. Parameter estimates from each trial-specific GLM were used to create a linear contrast image comparing the target decision period to the implicit baseline (unmodeled events). We then used the unthresholded z-statistics of this contrast to extract univariate and multivariate estimates of the BOLD signal in regions of interest.

Extracting Univariate ROI Activity from Single Trial Estimates (Classic Model). Masks were defined to extract univariate activity from the NAcc and lPFC. Both masks were defined using the Harvard-Oxford probabilistic atlas as rendered in FSL's viewer (fslview) on the MNI152 NLIN 6th generation T1 template image at 2 mm^3 voxel resolution (avg152T1_brain.nii.gz; 51). This atlas contains probabilistic masks to various bilateral structures that articulate the probability that a given voxel within the mask falls in the specified brain region. We created a bilateral NAcc mask by merging the atlas' left and right nucleus accumbens probabilistic images into a nifti volume and thresholding the image at $p = .25$. We selected the nucleus accumbens due to prior empirical and theoretical accounts of this region's importance in adolescent risk-taking (6,52). The .25 threshold was selected with the goal of creating a mask that was relatively inclusive but did not also possess clear outlying voxels (i.e.,

voxels with a very low probability of landing in the accumbens). A similar procedure was used to create a bivariate lPFC mask by selecting and merging left and right interior frontal gyrus masks (both the pars opercularis and pars triangularis) and thresholding the image at $p = .50$. We chose a .5 threshold for this mask because lPFC activation reported in prior adolescent neuroimaging studies tends to be spatially broad. However, we also created another version of this mask by thresholding at $p = .25$ in order to be consistent with the NAcc mask and found broadly consistent results (see Supplement).

Once our masks were defined, we transformed the masks into the native space for each single trial activity map using FLIRT (i.e., whole brain zstat) and then extracted activity estimates using the nilearn software package (53). We used the package's `NiftiMasker()` function to mask each single trial activity estimate with the aforementioned NAcc mask and then again with the aforementioned lPFC mask and extract the mean of all voxels within each respective mask (Figure 1C). It was at this step that we applied smoothing to the extracted data (6 mm, fwhm), as the `NiftiMasker()` function allows one to smooth a masked image when extracting data. This step produced a set of NAcc and lPFC activation estimates for each trial on the task across all subjects (i.e., each subject had as many NAcc and lPFC activation estimates as they did decisions in the YLG).

Computing Pattern Expression from Single Trial Estimates (Switchboard). We used pattern expression analyses to quantify the extent to which whole-brain patterns of brain activity corresponded to neural signatures of cognitive control and value-based computations (Figure 1C). Such an analysis allows one to determine how strongly a given pattern of brain activity is expressed as a function of a neural signature of interest (33,40,54). Neural signatures are thought to be the fingerprints of brain activity that encode a particular psychological process or state of interest. In practice, they are frequently defined as maps of the brain containing weights that quantify the strength and direction of association between each voxel and the psychological process of interest.

The first step in this analysis involved defining neural signatures of cognitive control and value-based computation. To this end, we used Neurosynth, a web-based platform that automates meta-analysis over a large set of published fMRI studies (55), to retrieve meta-analytic maps (uniformity) for the terms 'value' (470 studies) and 'cognitive control' (598 studies). We chose these terms based on system-based theories such that 'value' references one system which drives adolescents to make risky decisions in service of acquiring immediate hedonic rewards whereas 'cognitive control' references a second system which modulates the drive towards immediate rewards (3,7). A benefit of using meta-analytic maps as neural signatures is that they 'allow the data to speak for themselves' by allowing us to select voxels weights that are most strongly associated to our psychological processes of interest (in contrast to approaches that posit singular ROIs that might exclude meaningful voxels). To ensure the robustness of results, we used both

the uniformity and association maps (association reported in main text, uniformity reported in Supplementary Table 4A). While a review of the differences between these two types of images is beyond the scope of this paper (see Neurosynth.org/faq), we briefly note here that association maps provide greater selectivity about the relationship between a voxel and a given term by incorporating information about base rates. To be comprehensive, we re-ran all analyses with the Neurosynth term 'reward' and observed nearly identical results.

Once the neural signatures were defined, we transformed each signature into the native space of each single trial activity map (i.e., whole brain zstat), and extracted multivariate patterns from both the transformed neural signatures and activity estimates using `NiftiMasker()`. Multivariate patterns were minimally smoothed (1mm fwhm; 56) and then the dot product between voxels in the two patterns (activity estimate, neural signatures) was taken (we re-ran all analyses with a greater smoothing kernel–4mm fwhm–and obtained highly similar results). This resulted in two pattern expression estimates per trial, one quantifying the expression of value patterns in brain activity during a given decision and another quantifying the expression of cognitive control patterns in brain activity during the same decision. Barring missing decision data (See Figure 2), each subject had 90 pattern expression estimates - 45 for value and 45 for cognitive control, each corresponding to a decision during the yellow light game.

Notably, we were aware of previous work using pattern expression analyses with a preprocessing stream that involved normalizing images to standard space (40,54). We note that our decision to keep images in subject space for pattern expression calculation is not necessarily at odds or incompatible with these prior studies, best practices for pattern expression analyses, or even the broader MVPA literature. Unlike these prior studies, our goal was not to create a biomarker or construct a neural signature that can be applied across an entire population (56). Because our focus was on intra-individual fluctuations in activity and links to decision-making behavior, it was appropriate to refrain from normalizing to preserve fine-grain spatial information.

Between-Subject Analyses.

Aggregation of Trial-Level Data for Between-Subjects Analysis. In order to conduct between-subject analyses, we aggregated the trial-level univariate and pattern expression data. We did this by taking the average of the aforementioned brain activity metrics for each subject.

Group-Level Brain Mapping Analysis. We conducted traditional, group-level brain mapping (mass univariate) analyses to serve as a comparison point and complement our between-subject analyses (38,43,44). To this end, we first submitted each participant's run-level data to a fixed GLM analysis in FSL. For this purpose, the YLG was modeled consistent with other prior univariate studies (and consistent with our single trial analysis, to the extent possible) by including a regressor for 'Go' decisions, a regressor for 'Stop' decisions, and one for each

outcome (regardless of type, successful pass, pause, crash). The same pre-processing decisions steps were taken as in all other analyses (e.g., slice timing correction via adding temporal derivatives, adding extended motion parameters, censored volumes, etc.). The only exception was that we smoothed our data for this model (6mm, fwhm), and non-linearly registered high resolution anatomical images to the MNI152 template image (10 mm warp resolution), and used the subsequent transformation matrix to register the functional images to standard space.

Parameter estimates from this GLM were used to create linear contrast images comparing the 'Go' and 'Stop' conditions ('Go' - 'Stop', 'Stop-Go'). Random effects, group-level analyses were performed on this contrast using FSL's FLAME1 module. A cluster defining threshold of Z = 3.1 was used in conjunction with a familywise error rate of $p < 0.05$ and Random Field Theory cluster correction to address the problem of multiple comparisons. An additional whole-brain analysis regressed age (mean centered) on these contrasts.

Statistical Approach

Overview. Our analytic approach consisted of two parts. The first set of analyses examined neural systems underlying within-subject variability in decision making, using both classic and switchboard models. The second set of analyses examined between-subject variability in decision making. Here, we again compared classic and switchboard dual-systems models. A detailed description of both approaches follows below. For thoroughness, we also report a traditional between-subjects univariate analysis of the YLG in the supplement.

Within-Subjects: Modeling Trial-Level Influences of Brain on Behavior. We executed our within-subjects test of the classic and switchboard models with a series multilevel logistic regression models. For each theory (classic, switchboard), we conducted a multilevel logistic regression model including trial-level estimates of brain activity and subject level controls (age, gender). The form and specification of the statistical models for both variants follow.

Trial-level, Classic:

$$\text{Logit}(\text{Decision}_{ij}) = \pi_{0ij} + \pi_{1ij}(\text{NAcc}_{ij}) + \pi_{2j}(\text{lPFC}_{ij})$$

Trial-level, Switchboard:

$$\text{Logit}(\text{Decision}_{ij}) = \pi_{0ij} + \pi_{1ij}(\text{Value PE}_{ij}) + \pi_{2j}(\text{Cognitive Control PE}_{ij})$$

Decisions (1 = risky ('Go'), 0 = safe ('Stop')) at the *i*-th trial for the *j*-th individual were modeled as a function of a subject-specific intercept (π_{0ij}), and brain activity metrics. The brain

activity metrics in the classic model were average activations in the ventral striatum ($NAcc_{ij}$) and lateral prefrontal cortex ($lPFC_{ij}$) at the *i*-th trial for the *j*-th individual. Said activity metrics in the switchboard model were pattern expression (PE) estimates for value (Value PE_{ij}) and cognitive control (Cognitive Control PE_{ij}). Brain activity estimates in both models were standardized. Subject-specific parameters for all within-person predictors (π_{1ij} & π_{2ij}) correspond to the subject-specific expected change in the log odds of making a risky decision given a one unit increase in the predictor (e.g., average univariate brain activity, pattern expression score) holding the other predictors constant. All trial-level predictors were standardized using the grand mean.

As noted above, we controlled for the following between subject variables: gender (dummy coded, 0 = male, 1 = female) and age.[2] The form of the between subjects component of the model for both classic and switchboard follows (i.e., this component of the model was the same for both classic and switchboard models).

$$\pi_{0ij} = \gamma_{00} + \gamma_{01}(\text{Gender}_j) + \gamma_{02}(\text{Age}_j) + u_{0j}$$
$$\pi_{1ij} = \gamma_{10} + u_{1j}$$
$$\pi_{2ij} = \gamma_{20} + u_{2j}$$

This component of the model reflects how all trial-level terms are allowed to vary randomly between subjects (indicated the u_j's, random effects) while showing the main effect of between subject predictors (γ_{01} & γ_{02}). The other gammas in the model (γ_{10} & γ_{20}) represent the fixed effect of the trial-level predictors (i.e., the portion of trial-level effects that are common to all participants). Random coefficient regression models were implemented with the 'lme4' package in R (57) and significant tests were obtained using the 'lmerTest' package (58).

Modeling Between-Subject Brain-Behavior Associations. Using the aggregated univariate activity (i.e., the average of each subjects' trial-level brain activity metrics) and aggregated pattern expression estimates (obtained via averaging over estimates within each subject), we sought to examine between subject brain-behavior associations. To do so, we conducted two multiple regression analyses. The first analysis examined the contribution of univariate NAcc and lPFC activity on the percentage of risky decisions during the task, while controlling for age and gender. The second analysis swapped out the univariate predictors for the multivariate pattern expression metrics.

Results

[2] We also tested permutations of these models that allowed age to interact with the trial-level brain activity metrics, effectively testing the possibility that the strength of the two neural systems changes with age. All age X brain interactions were null.

Baseline Models and Descriptive Data Visualizations. Individual decisions across all subjects are plotted in Figure 2. This figure highlights the variability in risky behavior both within and between subjects. Additionally, we ran two 'baseline' multilevel logistic regression models on the trial-level risky decision-making data from the YLG. The first model was an empty model, modeling trial-level decisions only as a function of an intercept, effectively estimating the unconditional likelihood of making a risky decision on the task (Supplementary Table 2). The second model included gender and age as predictors so as to examine the effects of these variables unconditioned on the brain activity data (Supplementary Table 2)—neither were related to risky decision likelihoods.

Within Subjects Results. Results from our within-subject models are summarized in Tables 1 and 2, and Figure 3. Each are described in greater detail below.

Classic. Using the classic system-based model, we found that trial-level univariate NAcc and lPFC activity were independently associated with decision tendencies in the yellow light game in a manner consistent with theory. Within-person increases in NAcc activity were associated with an increased likelihood of making a risky decision, whereas within-person increases in lPFC activity were associated with a decreased likelihood of making a risky decision. The magnitude of the effects were comparable: a one unit increase in NAcc activity was associated with a 14.99% increase in the expected odds of making a risky decision, while a one unit increase in lPFC activity corresponded with a 15.84% decrease in the expected odds of making a risky decision (calculated using coefficients in Table 1). Notably, these results remained highly similar when using an alternate, more conservative lPFC mask (results still significant, same direction, comparable effect sizes; Supplementary Table 3).

Switchboard. Results from the switchboard system-based model are summarized in Table 2. These results are partially consistent with system-based theories, in that cognitive control pattern expression estimates were significantly associated with risky decision making on the YLG. A one unit increase in cognitive control pattern expression corresponded with a 13.09% decrease in the expected odds of making a risky decision (obtained from Table 2B). Sensitivity analyses indicated this effect was robust to variations in neural signatures (e.g., when using uniformity and association maps, unique voxels in uniformity maps, see Supplementary Table 4) and these effects were not present when using theoretically orthogonal neural signatures ('vision' and 'auditory', see Supplementary Table 5). Collectively these results indicate that multivariate pattern-based activity related to cognitive control encodes meaningful information about risk-taking tendencies. Simultaneously, and inconsistently with system-based theories, value-based pattern expression estimates were not significantly associated with risky decision propensities (coefficient: .051, (SE = .048, ns), from Table 2B). To ensure our value-based results were not driven via the selection of an erroneous pattern, we re-ran analyses using Neurosynth's 'reward' term and obtained near-identical results (reward coefficient: .043 (SE = .048, ns)). Importantly,

multivariate patterns and univariate activity metrics were modestly correlated (correlations ranged between approximately .09 and .4), and overlap between the lPFC and cognitive control multivariate signature—the only system that was significant in both model variants—was minimal (only 7.9% of the voxels in the cognitive control signature were also present in the lPFC mask). We reiterate here that univariate activity metrics and multivariate pattern expression scores represent different aspects of brain activity, and these descriptive statistics emphasize this point.

We conducted *post-hoc* analyses to interrogate the lack of a relationship between value-based pattern expression estimates and risky behavior. We first examined whether multivariate signatures within the NAcc were associated with behavior given that univariate signals within this region were, operating under the logic that value-based patterns may be more localized to a given region than cognitive control. We re-ran the pattern expression analyses with the value-based neural signature, but this time only included voxels in the NAcc in our mask. Again, this analysis showed a non-association between value-based pattern expression scores in the NAcc and risky decision making (γ_{01} = 0.000, *ns*). Given this result and the nature of pattern expression analysis, it was puzzling why univariate activity in the NAcc tracked with behavior (especially when considering a bulk of the pattern was comprised of NAcc voxels, see Supplemental Figure 4), but value-based signatures—even if localized to the NAcc—did not. This led us to believe that perhaps it was the homogeneity of multivariate activity in NAcc that related to risky decision tendencies. Multivariate patterns necessarily encode spatial variability, but it could that homogeneity or uniformity of activity are more strongly predictive of behavior, suggesting that pattern expression estimates that inherently capture this variability may be poor predictors of behavior. To test this, we re-extracted multivariate patterns from the NAcc and lPFC and computed Gini coefficients for each region for each trial. Traditionally used in macroeconomics but recently applied in neuroscience (59,60), Gini coefficients in this context can describe the extent to which brain activity in a given region is homogenous (uniform) or heterogeneous. Indeed, as shown in Supplementary Table 6, a lower Gini coefficient in the NAcc (i.e., more uniform activation) was associated with an increased propensity to take risks on the YLG, suggesting a strong, one-dimensional encoding of value signatures during decision-making.

Between Subject Results. Results from between subject analyses indicate that none of the between-subject brain activity metrics (univariate or pattern based) were related to proportion of risky decisions (univariate NAcc: b = 0.223, SE = 0.316, p > .250; univariate lPFC: b = -0.209, SE = 0.270, p > .250; value pattern expression: 8.725e-5, SE = 1.823e-4, p > .250; cognitive control pattern expression: -1.435e-4, SE = 1.219e-4, p = .245). A traditional brain mapping (mass univariate) analysis of the YLG showed significant anterior cingulate cortex (ACC) activity for the ‘Go > Stop’ contrast in addition to significant amygdala and dorsal striatal activity (Supplementary Table 7).

Discussion

The current study employed a brain modeling philosophy (33) in conjunction with within-subject multilevel logistic regression to test system-based theories of decision-making, using adolescent decision-making as an exemplar case. In doing so, we also expanded upon traditional neuroscientific implementations of system-based theories by examining the role of multivariate neural signals. We found that features of brain activity predicted behavior in a manner consistent with system-based theories. We observed this in two variants of the model—a classic implementation assuming modularity among ROIs, and a novel variant that included information for multivariate signatures. These findings have a number of ramifications for neuroscientific models of decision-making.

Implications for System-Based Theories of Decision-Making. We observed that value-based and cognitive control systems generally predicted behavior in a manner consistent with system-based theories: univariate estimates of NAcc and lPFC activity were directly and inversely, respectively, associated with the probability of making risky decision, while cognitive control pattern expression was predictive of a reduced likelihood to make a risky decision. Our between subject analyses, along with traditional mass univariate brain mapping analyses, failed to show any such trends. Two broad conclusions follow from these results. First, these findings support the utility of brain modeling techniques for testing system-based theories of decision-making in developmental neuroscience and beyond. This is unsurprising because such theories posit that the brain causally influences behavior at the level of the individual in the first place (i.e., within-subjects) (e.g., Steinberg, 2010), which is inconsistent with brain mapping. Nevertheless, our results reinforce that brain modeling and brain mapping philosophies are not simply inverse functions of the other that yield equivalent results (33). Second, and perhaps more importantly, these results suggest that system-based theories of decision-making have at least some evidentiary value, despite compelling arguments that they are too simplistic to be neurobiologically plausible (11,61). The present findings suggest that system-based theories may offer interim frameworks for relatively young fields such as cognitive neuroscience as they continue to incrementally extend theory on the basis of novel evidence (32,62). Even as these theories are eventually replaced by stronger and more nuanced accounts (e.g., 63), their use as 'baseline' models may actually facilitate novel theoretical insights so long as they are not subscribed to too rigidly.

The Role of Modularity and Population Coding for System-Based Theories of Decision-Making. On a more granular level, our results speak to two long-discussed concepts in human neuroimaging work: modularity and population coding (64). The former refers to the assumption that a single brain region executes a single, encapsulated function, whereas the latter refers to the idea that the brain distributes information across neurons via a code. These two concepts are respectively reflected by univariate and multivariate analyses in neuroimaging data. Most

system-based theories of decision-making originate from disciplines within psychological science that espoused modularity at the *psychological level* (14), especially in the domain of adolescent risk-taking. Although it is not a given that psychological modularity necessitates neural modularity, this assumption has been preserved in many neuroscientific system-based theories of adolescent decision making (3,12,17), despite evidence in adults that multivariate patterns reflect meaningful information about decision-making (65). Our univariate and multivariate results, somewhat surprisingly, respectively provide support for *both* modularity and population coding – specifically, our brain modeling approach revealed that univariate NAcc and lPFC activity was associated with decision behavior, and also that our multivariate cognitive control (but not value) pattern expression values predicted decision behavior. The former (evidence of modularity) is surprising, given the limited support for neural modularity that prior studies have found (64), whereas the latter (population coding) is notable because no prior studies, to our knowledge, have found evidence of such in the context of brain modeling decision behavior.

These findings carry a few notable implications. Although our results suggest that modularity may be a feature of adolescent decision behavior, we cannot conclude with certainty what activation in those modules (i.e., NAcc and lPFC) reflect. While such activation could index computations related to value and cognitive control, respectively, it is more difficult to infer psychological processes from ROI-based activity than from multivariate signatures, which tend to be more specific in what they reflect (54,66). Our data are consistent with an amplifier model, which would allow for reconciliation of our classic and switchboard results. In such a model, multivariate patterns may code for the psychological process of interest and the modules observed here act as 'volume' knobs that amplify their magnitude. Indeed, multidimensional coding schemes appear to support decision behaviors in monkeys (67), and thus may also be plausible in humans. It is clear that much additional work is needed to characterize the relative contributions of neural modules and population codes in system-based theories of decision-making, involving the use of different behavioral tasks, different modules (though see our sensitivity analyses in the supplement) and multivariate signatures, and evaluating decision behaviors in different contexts.

Building on System-Based Theories of Decision-Making. Our findings suggest that system-based models provide at least some explanatory utility but it is critical that future work improves upon existing models in several key ways. One future step will be to determine the algebraic form of influential system-based theories. As we noted before, existing neuroscientific system-based theories of human decision making in linguistic terms without specifying a computational model (i.e., they are explained qualitatively, instead of with an algebraic equation). This means that one could posit a number of algebraic forms that satisfy qualitative requirements of system-based theories that each carry very different implications. Here we assumed a linear relationship between the log odds of a risky choice and metrics of brain

activity, but an alternate statistical model may be more appropriate. Future studies may seek to test a set of candidate algebraic formulations of system-based theories of decision-making (e.g., probit, estimating latent value and linking to decision likelihoods, etc.). Doing so will facilitate cross-study and cross-discipline comparison by setting an objective framework that supports falsifiability. Future work will also need to directly address our null findings involving value-based pattern expression values. While we tested both 'reward' and 'value' patterns and obtained null results with both, it is possible that an alternative untested pattern computed in a different manner (i.e., not relying on meta-analytic maps) would yield positive results. To rigorously test this possibility, we recommend that future studies systematically create and test patterns that vary iteratively on psychological processes relevant for system-based theories (40,54). Taking such an approach would have the added benefit of providing insights into what specific psychological features these patterns encompass – for example, by examining subcomponents of cognitive control (e.g., inhibition/selection, working memory, etc.).

Limitations and future directions. The current study has several limitations that point directly to future directions in this line of research. The first is that the effect sizes found from key results are somewhat modest. Though not a traditional 'limitation' per se, this points to the possibility that other untested computational signals in the brain may also contribute to decision behavior. Another limitation is that the present results were obtained in a single, moderately-sized sample and ought to be replicated (68,69). That said, our concerns about samples size are partially assuaged by the fact that we leveraged multilevel models to maximize statistical power when examining brain-behavior associations (70). Two potential limitations also exist regarding generalizability. First, in terms of adolescent decision-making, prior work shows adolescent decision behaviors are prone to tremendous diversity across the world and even within individuals (20), forcing us to consider that these results, even ignoring other limitations, may not reflect a 'common ground truth' among all humans or even within a single human (to the extent such a ground truth actually exists). Second, it is possible that a different pattern of results would emerge for decision behaviors in other contexts (e.g., moral, financial decisions). A final limitation is that we did not compare our implementation of system-based theories to alternative theories. While this is mainly because system-based theories have dominated the field and alternative approaches have been relatively atheoretical (11,32), we look forward to future work aimed at rigorously comparing alternate explanations.

Concluding Remarks. System-based theories of decision-making have drawn tremendous scholarly interest, yet the veracity of their neuroscientific implementation has been the subject of much debate. This investigation was the first to our knowledge to test system-based theories of decision-making using a brain modeling approach, representing a methodological approach that is more consistent with the core tenets of such theories. We found evidence that system-based theories are indeed predictive of risk-taking behaviors, showing that univariate and multivariate brain activity metrics of cognitive control and value-based processes predict trial-by-trial risky

decision tendencies. Overall, this work contributes knowledge about the neural bases of decision behavior.

Table 1. Log-odds of risky choice from within-subjects analysis of classic system-based models

Term	Estimate
Intercept	0.580 (0.121)***
NAcc	0.140 (0.063)*
lPFC	-0.147 (0.057)*
Age	0.105 (0.086)
Gender	-0.084 (0.172)
Variance Component	**Estimate**
Var(π_{0ij})	0.267
Var(π_{1ij})	0.041
Var(π_{2ij})	0.024
Fit Statistic	**Statistic**
AIC	2888.7
BIC	2951.5

Note. ‘ refers to $p < .10$, * refers to $p < .05$, ** refers to $p < .01$, *** refers to $p < .001$. Gender was dummy coded (0 = male, 1 = female). NAcc refers to univariate ventral striatum activity; lPFC refers to univariate lateral prefrontal cortex activity. Var() refers to a variance component of a given random effect from the model. Results come from a multilevel logistic regression model, with log-odds of a risky choice as the dependent variable.

Table 2. Log-odds of risky choice from within-subjects analysis of switchboard system-based models

Term	Estimate
Intercept	0.581 (0.123)***
Value PE	0.051 (0.048)
Cognitive Control PE	-0.123 (0.047)**
Age	0.113 (0.087)
Gender	-0.104 (0.181)
Variance Component	**Estimate**
Var(π_{0ij})	0.259
Var(π_{1ij})	0.000
Var(π_{2ij})	0.003
Fit Statistic	**Statistic**
AIC	2894.3
BIC	2957.1

Note. ‘ refers to $p < .10$, * refers to $p < .05$, ** refers to $p < .01$, *** refers to $p < .001$. Value PE refers to value-based pattern expression; Cognitive Control PE refers to cognitive control pattern expression. Pattern expression analyses from these models were conducted using the association maps from Neurosynth. Var() refers to a variance component of a given random effect from the model. Results come from a multilevel logistic regression model, with log-odds of a risky choice as the dependent variable.

Figure 1. Schematic of Data Collection, Processing, and Analysis

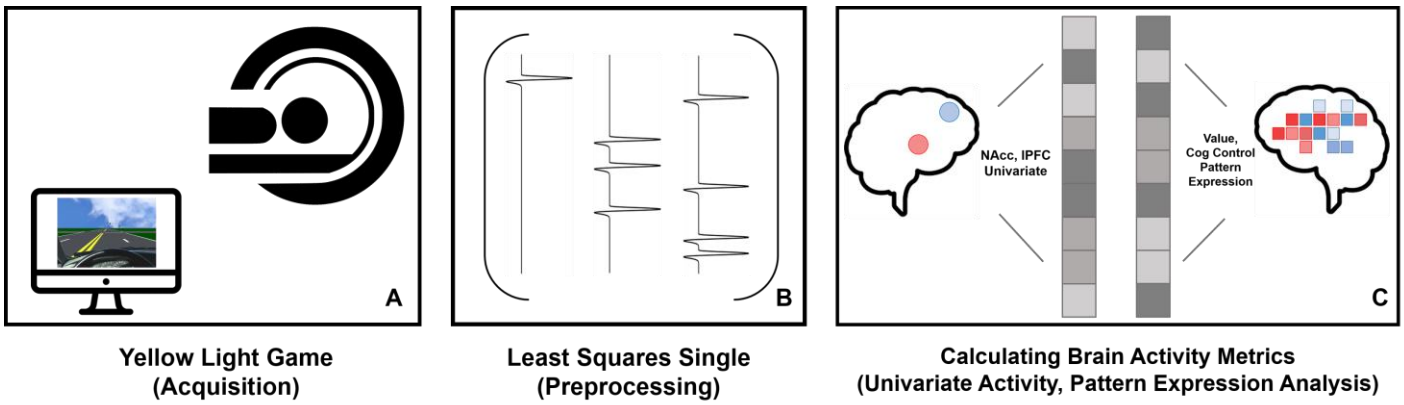

Note. Panel A depicts data acquisition of the Yellow Light Game while participants were undergoing fMRI scanning. Panel B depicts the Least Squares Single (LSS) modeling implemented as a preprocessing step. Panel C is a schematic of extracting univariate and multivariate data from the beta-series that resulted from the LSS modeling in Panel B.

Figure 2. Visualizing risky and safe decisions on the yellow light game for all participants

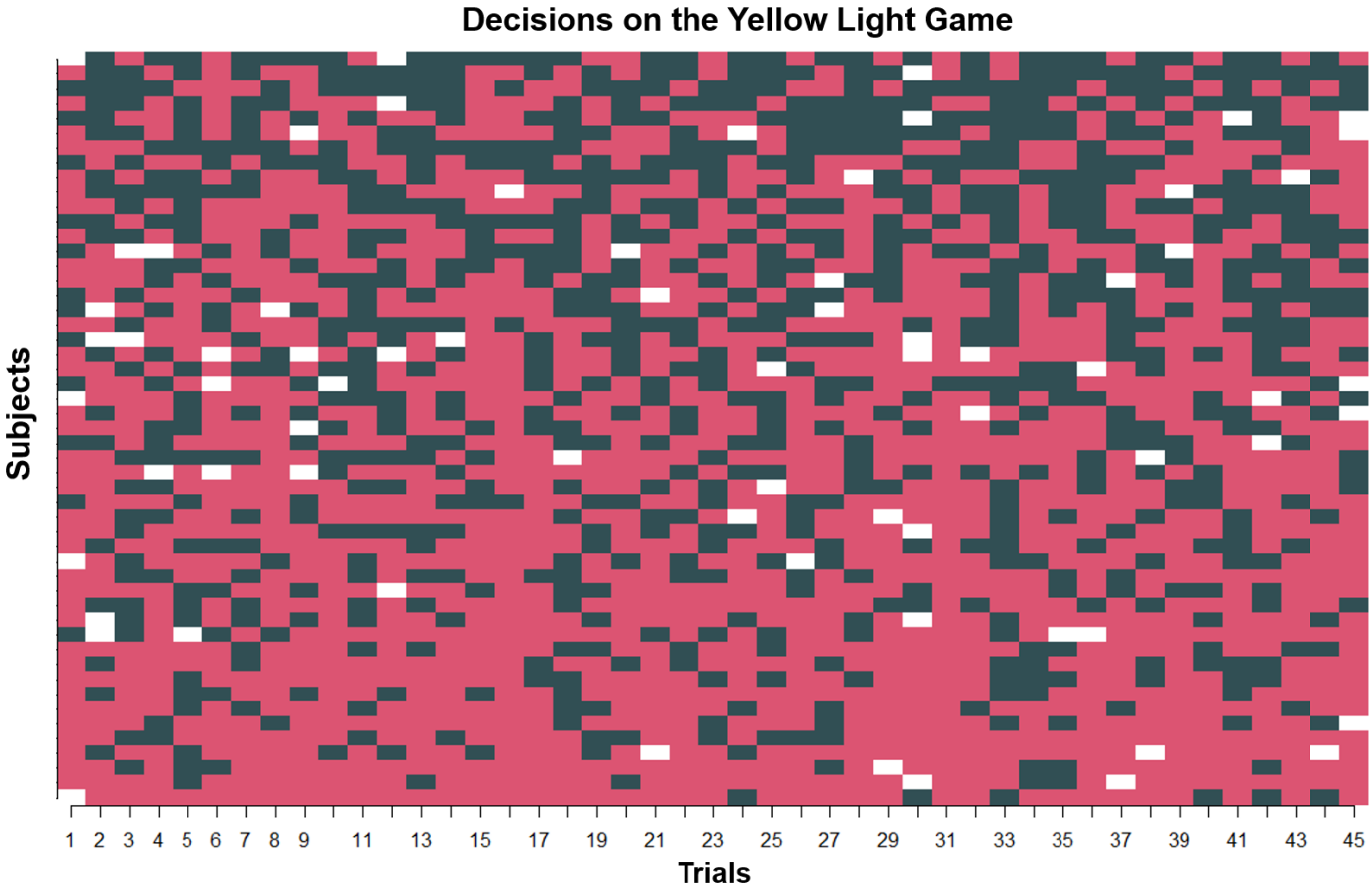

Note. Red squares represent risky decisions, black squares represent safe decisions, white squares represent no decision (i.e., failure to respond). Columns correspond to decision (trial) number, arranged chronologically; Rows correspond to subjects (arranged in order of descending rate of risky decisions). Entries into the matrix represent whether a given subject made a risky or safe decision on a given trial.

Figure 3. Associations between univariate and multivariate brain activity and probability of making a risky decision

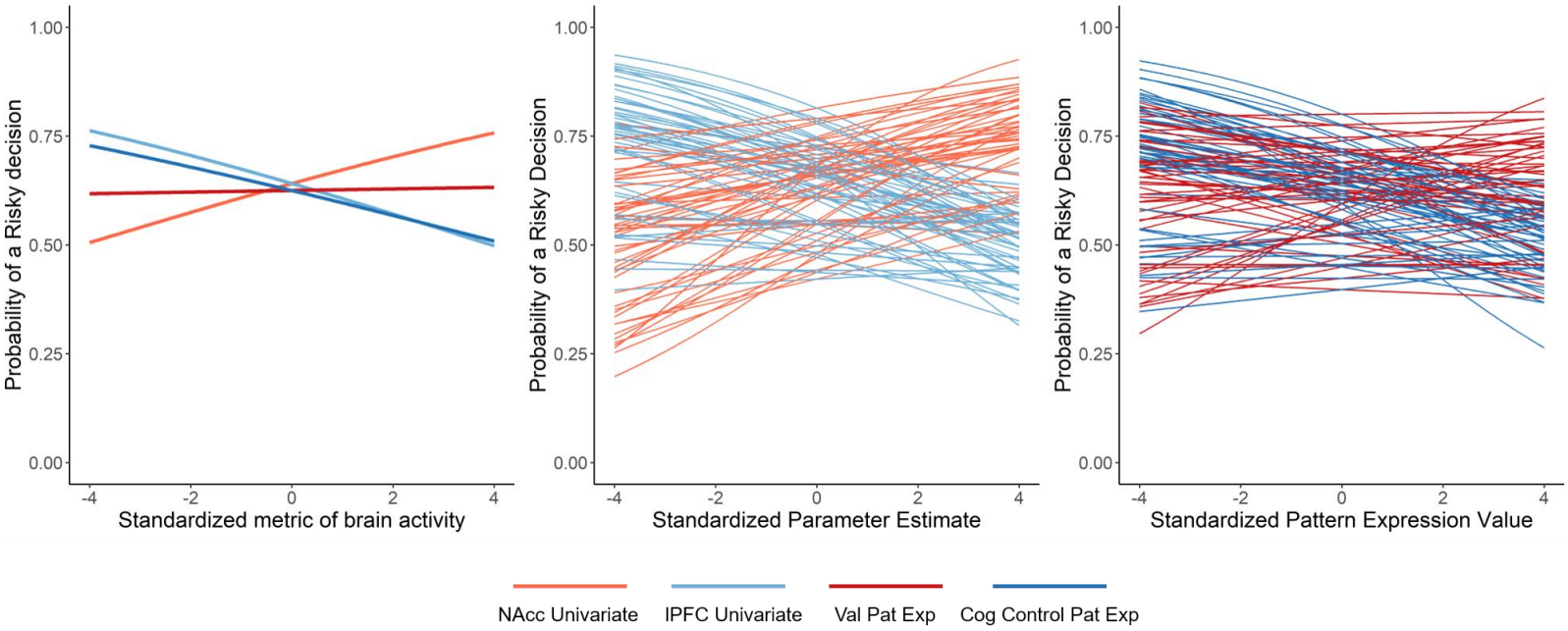

Note. 'NAcc Univariate' refers to the trial-level univariate NAcc activity estimates; 'lPFC Univariate' refers to the trial-level univariate lPFC activity estimates; 'Cog Control Pat Exp' refers to trial-level cognitive control pattern expression estimates; 'Value Pat Exp' refers to trial-level value-based pattern expression estimates. Fixed effects of brain activity metrics from both models are shown in the left panel. Subject specific random effects of associations between risky decision-making probability and univariate NAcc and univariate lPFC activity are depicted in the middle panel. Subject specific random effects of associations between risky decision-making probability and, value-based pattern expression, and cognitive control pattern expression values are depicted in the right panel.

Acknowledgments. Preparation of this manuscript was supported by a National Science Foundation Graduate Research Fellowship (2016220797) and a National Institutes of Health Predoctoral T32 Fellowship to JFGM, and generous funds from the UCLA academic senate, UCLA Hellman Fellows Fund, and an NSF CAREER grant (1848004), to JAS. We thank Drs. Jennifer Pfeifer and Shannon Peake for sharing the Yellow Light Game with us. We appreciate the efforts of Austin Blake, Alejandra Delgado, Zoey Dew, Milagro Escobar, Elizabeth Gaines, Agatha Handojo, Ciara Mandich, Nora Ngo, Sakina Qadir, Emily Towner, Claire Waller, and Tarran Walter in participant recruitment and data collection. We are grateful for reflections on the study concept from Dr. Jamie Feusner, Dr. Andrew Fuligni, Dr. Adriana Galván, Amanda E. Baker, Zoe Guttman, and Dr. Monica Rosenberg's Cognition, Attention, and Brain Lab at the University of Chicago.

References

1. Glimcher PW. Decisions, uncertainty, and the brain: The science of neuroeconomics. MIT Press; 2004.
2. Casey BJ. Beyond simple models of self-control to circuit-based accounts of adolescent behavior. Annu Rev Psychol [Internet]. 2015;66:295–319. Available from: http://www.ncbi.nlm.nih.gov/pubmed/25089362
3. Shulman EP, Smith AR, Silva K, Icenogle G, Duell N, Chein J, et al. The dual systems model: Review, reappraisal, and reaffirmation. Dev Cogn Neurosci [Internet]. 2016;17:103–17. Available from: http://dx.doi.org/10.1016/j.dcn.2015.12.010
4. O'Doherty JP. Reward representations and reward-related learning in the human brain: insights from neuroimaging. Curr Opin Neurobiol. 2004;14(6):769–76.
5. Tversky A, Kahneman D. Advances in prospect theory: Cumulative representation of uncertainty. J Risk Uncertain. 1992;5:297–323.
6. Steinberg L. A dual systems model of adolescent risk-taking. Dev Psychobiol. 2010;52(3):216–24.
7. Steinberg L. The influence of neuroscience on US Supreme Court decisions about adolescents' criminal culpability. Nat Rev Neurosci [Internet]. 2013;14(7):513–8. Available from: http://www.ncbi.nlm.nih.gov/pubmed/23756633
8. Gantman AP, Van Bavel JJ. Moral Perception. Trends Cogn Sci [Internet]. 2015;19(11):631–3. Available from: http://dx.doi.org/10.1016/j.tics.2015.08.004
9. Yoder KJ, Decety J. The neuroscience of morality and social decision-making. Psychol Crime Law. 2018;24(3):279–95.
10. Gouret F, Hollard G. When Kahneman meets Manski: Using dual systems of reasoning to interpret subjective expectations of equity returns. J Appl Econom. 2011;26(3):371–92.
11. Pfeifer JH, Allen NB. Arrested Development? Reconsidering dual-systems models of brain function in adolescence and disorders. Trends Cogn Sci. 2012;16(6):322–9.
12. Luciana M, Wahlstrom D, Porter JN, Collins PF. Dopaminergic modulation of incentive motivation in adolescence: Age-related changes in signaling, individual differences, and implications for the development of self-regulation. Dev Psychol. 2012;48(3):844–61.
13. Silverman MH, Jedd K, Luciana M. Neural networks involved in adolescent reward processing: An activation likelihood estimation meta-analysis of functional neuroimaging studies. Neuroimage [Internet]. 2015;122:427–39. Available from: http://dx.doi.org/10.1016/j.neuroimage.2015.07.083
14. Steinberg L, Albert D, Cauffman E, Banich M, Graham S, Woolard J. Age differences in sensation seeking and impulsivity as indexed by behavior and self-report: Evidence for a dual systems model. Dev Psychol [Internet]. 2008;44(6):1764–78. Available from: http://psycnet.apa.org/psycinfo/2008-16008-019%5Cnhttp://www.ncbi.nlm.nih.gov/pubmed/18999337
15. Cohen AO, Casey BJ. Rewiring juvenile justice: The intersection of developmental neuroscience and legal policy. Trends Cogn Sci [Internet]. 2014;18(2):63–5. Available from: http://dx.doi.org/10.1016/j.tics.2013.11.002
16. Yeager DS, Dahl RE, Dweck CS. Why interventions to influence adolescent behavior often fail but could succeed. Perspect Psychol Sci. 2018;13(1):101–22.
17. Strang NM, Chein JM, Steinberg L. The value of the dual systems model of adolescent risk-taking. Front Hum Neurosci [Internet]. 2013;7(May):223. Available from: http://www.pubmedcentral.nih.gov/articlerender.fcgi?artid=3664310&tool=pmcentrez&re

ndertype=abstract
18. Ernst M, Pine DS, Hardin M. Triadic model of the neurobiology of motivated behavior in adolescence. Psychol Med. 2006;36(3):299–312.
19. Rivers SE, Reyna VF, Mills B. Risk taking under the influence: A fuzzy-trace theory of emotion in adolescence. Dev Rev. 2008;28(1):107–44.
20. Steinberg L, Icenogle G, Shulman EP, Breiner K, Chein J, Bacchini D, et al. Around the world, adolescence is a time of heightened sensation seeking and immature self-regulation. Dev Sci [Internet]. 2017;([EPub Ahead of Print]):1–13. Available from: http://doi.wiley.com/10.1111/desc.12532
21. Botdorf M, Rosenbaum GM, Patrianakos J, Steinberg L, Chein JM. Adolescent risk-taking is predicted by individual differences in cognitive control over emotional, but not non-emotional, response conflict. Cogn Emot [Internet]. 2016;1–8. Available from: http://www.tandfonline.com/doi/full/10.1080/02699931.2016.1168285
22. Ellingson JM, Corley R, Hewitt JK, Friedman NP. A prospectie study of alcohol involvement and the dual-systems model of adolescent risk-taking during late adolescence and emerging adulthood. Addiction. 2019;114(4):653–61.
23. Forrest W, Hay C, Widdowson AO, Rocque M. Development of impulsivity and risk-seeking: Implications for the dimensionality and stability of self-control. Criminology. 2019;57(3):512–43.
24. Duell N, Steinberg L, Icenogle G, Chein J, Chaudhary N, Di Giunta L, et al. Age patterns in risk taking across the world. J Youth Adolesc. 2017;
25. Flannery JE, Giuliani NR, Flournoy JC, Pfeifer JH. Neurodevelopmental changes across adolescence in viewing and labeling dynamic peer emotions. Dev Cogn Neurosci. 2017;25:113–27.
26. Lee NC, Weeda WD, Insel C, Somerville LH, Krabbendam L, Huizinga M. Neural substrates of the influence of emotional cues on cognitive control in risk-taking adolescents. Dev Cogn Neurosci. 2018;31:20–34.
27. McIlvain G, Clements RG, Magoon EM, Spielberg JM, Telzer EH, Johnson CL. Viscoelasticity of reward and control systems in adolescent risk taking. Neuroimage. 2020;215.
28. van Duijvenvoorde ACK, Achterberg M, Braams BR, Peters S, Crone EA. Testing a dual-systems model of adolescent brain development using resting-state connectivity analyses. Neuroimage [Internet]. 2016;124:409–20. Available from: http://dx.doi.org/10.1016/j.neuroimage.2015.04.069
29. Romer D, Reyna VF, Satterthwaite T. Beyond stereotpes of adolescent risk taking: Placing the adolescent brain in developmental context. Dev Cogn Neurosci. 2017;27:19–34.
30. van Duijvenvoorde ACK, Peters S, Braams BR, Crone EA. What motivates adolescents? Neural responses to rewards and their influence on adolescets' risk taking, learning, and cognitive control. Neurosci Biobehav Rev. 2016;70:135–47.
31. McCormick EM, Gates KM, Telzer EH. Model-based network discovery of developmental and performance-related differences during risky decision-making. Neuroimage. 2019;188:456–64.
32. Pfeifer JH, Allen NB. The audacity of Specificity: Moving adolescence developmental neuroscience towards more powerful scientific paradigms and translatable models. Dev Cogn Neurosci. 2016;17:131–7.

33. Kragel PA, Koban L, Barrett LF, Wager TD. Representation, Pattern Information, and Brain Signatures: From Neurons to Neuroimaging. Neuron [Internet]. 2018;99(2):257–73. Available from: https://doi.org/10.1016/j.neuron.2018.06.009
34. Kanwisher N. The quest for the FFA and where it led. J Neurosci [Internet]. 2017;37(5):1056–61. Available from: http://www.jneurosci.org/lookup/doi/10.1523/JNEUROSCI.1706-16.2016
35. Zhao W, Palmer CE, Thompson WK, Chaarani B, Garavan HP, Casey BJ, et al. Individual differences in cognitive performance are better predicted by global rather than localized BOLD activity patterns across the cortex. Cereb Cortex. 2020;1–11.
36. Rudolph MD, Miranda-Domínguez O, Cohen AO, Breiner K, Steinberg L, Bonnie RJ, et al. At risk of being risky: The relationship between "brain age" under emotional states and risk preference. Dev Cogn Neurosci [Internet]. 2017;24:93–106. Available from: http://dx.doi.org/10.1016/j.dcn.2017.01.010
37. Redcay E, Warnell KR. A social-interactive neuroscience approach to understanding the developing brain. Adv Child Dev Behav. 2018;54:1–44.
38. Telzer EH, Ichien NT, Qu Y. Mothers know best: Redirecting adolescent reward sensitivity toward safe behavior during risk taking. Soc Cogn Affect Neurosci. 2015;10(10):1383–91.
39. Cosme D, Ludwig RM, Berkman ET. Comparing two neurocognitive models of self-control during dietary restrictions. Soc Cogn Affect Neurosci. 2019;14(9):957–66.
40. Chang LJ, Gianaros PJ, Manuck SB, Krishnan A. A sensitive and specific neural signature for picture-induced negative affect. PLOS Biol. 2015;13(6):1–28.
41. Parkinson C, Kleinbaum AM, Wheatley T. Spontaneous neural encoding of social network position. Nat Hum Behav [Internet]. 2017;1(5):1–7. Available from: http://dx.doi.org/10.1038/s41562-017-0072
42. Huth AG, Heer WA De, Griffiths TL, Theunissen FE, Gallant JL. Natural speech reveals the semantic maps that tile human cerebral cortex. Nature. 2016;532(7600):453–8.
43. Op de Macks ZA, Flannery JE, Peake SJ, Flournoy JC, Mobasser A, Alberti SL, et al. Novel insights from the Yellow Light Game: Safe and risky decisions differentially impact adolescent outcome-related brain function. Neuroimage. 2018;181:568–81.
44. Chein JM, Albert D, O'Brien L, Uckert K, Steinberg L. Peers increase adolescent risk taking by enhancing activity in the brain's reward circuitry. Dev Sci. 2011;14(2):1–10.
45. Gardner M, Steinberg L. Peer influence on risk taking, risk preference, and risky decision making in adolescence and adulthood: An experimental study. Dev Psychol [Internet]. 2005;41(4):625–35. Available from: http://dx.doi.org.esc-web.lib.cbs.dk/10.1037/a0026993
46. Peake SJ, Dishion TJ, Stormshak EA, Moore WE, Pfeifer JH. Risk-taking and social exclusion in adolescence: Neural mechanisms underlying peer influences on decision-making. Neuroimage [Internet]. 2013;82:23–34. Available from: http://dx.doi.org/10.1016/j.neuroimage.2013.05.061
47. Greve DN, Fischl B. Accurate and robust brain image alignment using boundary-based registration. Neuroimage. 2009;48(1):63–72.
48. Rissman J, Gazzaley A, D'Esposito M. Measuring functional connectivity during distinct stages of a cognitive task. Neuroimage. 2004;23(2):752–63.
49. Mumford JA, Turner BO, Ashby FG, Poldrack RA. Deconvolving BOLD activation in event-related designs for multivoxel pattern classification analyses. Neuroimage

[Internet]. 2012;59(3):2636–43. Available from: http://dx.doi.org/10.1016/j.neuroimage.2011.08.076
50. Mumford JA, Davis T, Poldrack RA. The impact of study design on pattern estimation for single-trial multivariate pattern analysis. Neuroimage [Internet]. 2014;103:130–8. Available from: http://dx.doi.org/10.1016/j.neuroimage.2014.09.026
51. Brett M, Johnsrude IS, Owen AM. The problem of functional localization in the human brain. Nat Rev Neurosci. 2002;3(3):243–9.
52. Galvan A, Hare T a, Parra CE, Penn J, Voss H, Glover G, et al. Earlier development of the accumbens relative to orbitofrontal cortex might underlie risk-taking behavior in adolescents. J Neurosci. 2006;26(25):6885–92.
53. Abraham A, Pedregosa F, Eickenberg M, Gervais P, Mueller A, Kossaifi J, et al. Machine learning for neuroimaging with scikit-learn. Front Neuroinform. 2014;8:1–10.
54. Wager TD, Atlas LY, Lindquist MA, Roy M, Woo C-W, Kross E. An fMRI-based neurologic signature of physical pain. N Engl J Med. 2013;368(15):1388–97.
55. Yarkoni T, Poldrack RA, Nichols TE, Van Essen DC, Wager TD. Large-scale automated synthesis of human functional neuroimaging data. Nat Methods. 2011;8(8):665–70.
56. Weaverdyck ME, Lieberman MD, Parkinson C. Multivoxel pattern analysis in fMRI: a practical introduction for social and affective neuroscientists. Soc Cogn Affect Neurosci. 2020;15(4):487–508.
57. Bates D, Mächler M, Bolker BM, Walker SC. Fitting linear mixed-effects models using lme4. arXiv. 2014;1–51.
58. Kuznetsova A, Brockhoff PB, Christensen RHB. lmerTest package: Tests in linear mixed effects. J Stat Softw. 2017;82(13):1–26.
59. Guest O, Love BC. What the success of brain imaging implies about the neural code. Elife. 2017;6:1–16.
60. Guassi Moreira JF, McLaughlin KA, Silvers JA. Spatial and temporal cortical variability track with age and affective experience during emotion regulation in youth. Dev Psychol. 2019;55(9):1921–37.
61. Van Bavel JJ, Xiao YJ, Cunningham WA. Evaluation is a dynamic process: moving beyond dual system models. Soc Personal Psychol Compass. 2012;6:438–54.
62. Baddeley A. Working memory: Theories, models, and controversies. Annu Rev Psychol [Internet]. 2012;63(1):1–29. Available from: http://www.annualreviews.org/doi/10.1146/annurev-psych-120710-100422
63. Paige Harden K, Kretsch N, Mann FD, Herzhoff K, Tackett JL, Steinberg L, et al. Beyond dual systems: A genetically-informed, latent factor model of behavioral and self-report measures related to adolescent risk-taking. Dev Cogn Neurosci [Internet]. 2017;25:221–34. Available from: http://dx.doi.org/10.1016/j.dcn.2016.12.007
64. Erickson RP. The evolution and implications of population and modular neural coding ideas. Prog Brain Res. 2001;130:9–29.
65. Hampton JP, O'Doherty JP. Decoding the neural substrates of reward-related decision making with functional MRI. Proc Natl Acad Sci. 2007;104(4):1377–82.
66. Poldrack RA. Can cognitive processes be inferred from neuroimaging data. Trends Cogn Sci. 2006;10(2):59–63.
67. Zhang K, Chen CD, Monosov IE. Novelty, salience, and surprise timing are signaled by neurons in the basal forebrain. Curr Biol. 2019;29(1):134–42.
68. Marek AS, Tervo-Clemmens B, Calabro FJ, Montez DF, Kay BP, Hatoum AS, et al.

Towards reproducible brain-wide association studies. bioRxiv. 2020;1–40.
69. Helmer M, Warrington S, Mohammadi-Nejad A-R, Ji JL, Howell A, Rosand B, et al. On stability of canonical correlation analysis and partial least squares with application to brain-behavior associations. bioRxiv. 2020;1–43.
70. Mathieu JE, Aguinis H, Culpepper SA, Chen G. Understanding and estimating the power to detect cross-level interaction effects in multilevel modeling understanding and estimating the power to detect cross-level interaction effects in multilevel modeling. J Appl Psychol. 2012;97(5):951–66.
71. Kinghorn A, Shanaube K, Toskas E, Cluver L, Bekker LG. Defining adolescence: Priorities from a global health perspective. Lancet Child Adolesc Heal. 2018;2(5):e10.

Supplement

Revisiting the Neural Architecture of Decision Making: Univariate and Multivariate Evidence for System-Based Models in Adolescence

Guassi Moreira et al.

Supplementary Table 1. Head motion statistics

	n Volumes > 0.9mm (mean, SD)	Most extreme displacement (mean, SD)	% *n* Volumes < 0.9mm	% Extreme displacements < 1.8mm
Run 1	0.0816, 0.5714	0.3270, 0.2894	97.96%	100%
Run 2	0.2653, 0.8845	0.5013, 0.7125	87.76%	95.92%
Run 3	0.3265, 1.1617	0.4342, 0.4876	91.84%	95.92%

Note. '*n* Volumes > 0.9mm' reflects the average number of volumes exceeding the 0.9mm frame displacement threshold across subjects; 'Most extreme displacement' reflects the average of the most extreme frame displacements across subject. '% *n* Volumes < 0.9mm' indicates the percentage of subjects whose data did not have a single volume exceeding our 0.9mm frame displacement cut-off. '% Extreme displacements < 1.8mm' indicates the percentage of subjects whose most extreme frame displacement value did not exceed 1.8mm, corresponding to twice the value of our 0.9 mm threshold.

Supplementary Table 2. Log-odds of risky choice from Empty and Covariate-Only models

	Empty	Covariate-Only
Term	Estimate	
Intercept	0.527 (0.087)***	0.599 (0.119)***
Trial Number	-	-0.009 (0.047)
Age	-	0.104 (0.085)
Gender	-	-0.144 (0.169)
Variance Component	Estimate	
Var(Intercept)	0.282	0.268
Var(Trial Number)	-	0.006
Fit Statistic	Statistic	
AIC	2887.1	2892.8
BIC	2898.5	2932.8

Note. ‘ refers to $p < .10$, * refers to $p < .05$, ** refers to $p < .01$, *** refers to $p < .001$. Sex was dummy coded (0 = male, 1 = female). Standard errors of parameter estimates are printed in parentheses. Var() refers to a variance component of a given random effect from the model.

Supplementary Table 3. Log-odds of risky choice from classic within-subjects model with alternate lPFC mask

Term	Estimate
Intercept	0.575 (0.121)***
NAcc	0.135 (0.064)*
lPFC	-0.123 (0.058)*
Age	0.104 (0.086)
Gender	-0.077 (0.172)
Variance Component	**Estimate**
Var(π_{0ij})	0.267
Var(π_{1ij})	0.043
Var(π_{2ij})	0.024
Fit Statistic	**Statistic**
AIC	2888.7
BIC	2951.5

Note. ‘ refers to $p < .10$, * refers to $p < .05$, ** refers to $p < .01$, *** refers to $p < .001$. Gender was dummy coded (0 = male, 1 = female). NAcc refers to univariate ventral striatum (NAcc) activity; lPFC refers to univariate lateral prefrontal cortex activity. lPFC activity for these models came from an alternate mask whose boundaries were more conservative and thus covered less cortical space. Var() refers to a variance component of a given random effect from the model. Results come from a multilevel logistic regression model, with log-odds of a risky choice as the dependent variable.

Supplementary Table 4. Log-odds of risky choice from within-subjects analysis of switchboard model with unique voxels only

A.

Term	Estimate
Intercept	0.510 (0.122)***
Value PE	0.008 (0.054)
Cognitive Control PE	-0.119 (0.060)*
Age	0.134 (0.079)’
Gender	0.054 (0.181)
Variance Component	**Estimate**
Var(π_{0ij})	0.253
Var(π_{1ij})	0.006
Var(π_{2ij})	0.039
Fit Statistic	**Statistic**
AIC	2892.6
BIC	2955.4

B.

Term	Estimate
Intercept	0.619 (0.122)***
Value PE	-0.004 (0.052)
Cognitive Control PE	-0.154 (0.055)**
Age	0.122 (0.087)
Gender	-0.176 (0.174)
Variance Component	**Estimate**
Var(π_{0ij})	0.284
Var(π_{1ij})	0.010

Var(π_{2ij})	0.022

Fit Statistic	Statistic
AIC	2888.1
BIC	2950.9

Note. ‘ refers to $p < .10$, * refers to $p < .05$, ** refers to $p < .01$, *** refers to $p < .001$. Gender was dummy coded (0 = male, 1 = female). Value PE refers to value-based pattern expression; Cognitive Control PE refers to cognitive control pattern expression. Pattern expression analyses from panel A were conducted with uniformity maps; Analyses from panel B were conducted using only unique voxels among the value and cognitive control Neurosynth uniformity images (i.e., voxels that the two masks shared in common were removed). Var() refers to a variance component of a given random effect from the model. Results come from a multilevel logistic regression model, with log-odds of a risky choice as the dependent variable.

Supplementary Table 5. Log-odds of risky choice from models with additional Neurosynth patterns to gauge uniqueness of cognitive control pattern expression findings

Term	Estimate
Intercept	0.569 (0.120)***
Vision PE	0.096 (0.054)’
Auditory PE	0.075 (0.050)
Age	0.072 (0.083)
Gender	-0.072 (0.168)
Variance Component	**Estimate**
Var(π_{0ij})	0.292
Var(π_{1ij})	0.027
Var(π_{2ij})	0.011
Fit Statistic	**Statistic**
AIC	2888.4
BIC	2951.2

Note. ‘ refers to $p < .10$, * refers to $p < .05$, ** refers to $p < .01$, *** refers to $p < .001$. Gender was dummy coded (0 = male, 1 = female). The alternate maps correspond to the terms listed in the table (‘Vision’, ‘Auditory’). ‘PE’ refers to pattern expression. Association maps for each term were used. Var() refers to a variance component of a given random effect from the model. Results come from a multilevel logistic regression model, with logodds of a risky choice as the dependent variable.

Supplementary Table 6. Models with predicting decision activity from trial-level Gini coefficients

Term	Estimate
Intercept	0.629 (0.121)***
NAcc Gini	-0.115 (0.048)*
lPFC Gini	0.057 (0.047)
Age	0.080 (0.088)
Gender	-0.198 (0.172)
Variance Component	**Estimate**
Var(π_{0ij})	0.270
Var(π_{1ij})	0.009
Var(π_{2ij})	0.004
Fit Statistic	**Statistic**
AIC	2894.1
BIC	2956.9

Note. ‘ refers to $p < .10$, * refers to $p < .05$, ** refers to $p < .01$, *** refers to $p < .001$. Gender was dummy coded (0 = male, 1 = female). Var() refers to a variance component of a given random effect from the model. Results come from a multilevel logistic regression model, with log-odds of a risky choice as the dependent variable.

Supplementary Table 7. Brain regions which showed significant activation Go > Stop and Stop > Go.

Region		x	y	z	Z	k
Go > Stop						
Occipital Pole	L	-18	-90	0	7.51	13177[a]
Striatum	R	10	6	8	4.22	[a]
pSTS	L	-52	-36	28	5.18	491
ACC	R	12	10	42	5.15	406
Amygdala	L	-30	-10	-14	5.60	372
Amygdala	R	30	-12	-12	5.86	229
Insular Cortex	L	-56	4	12	4.49	216
SPL	R	24	-52	56	5.34	146
Stop > Go						
TPJ	R	50	-56	42	4.97	566
TPJ	L	-46	-60	46	4.52	204

Note. R refers to right and L refers to left. x, y, and z refer to MNI coordinates; Z refers to the z-statistic at those coordinates (local maxima); pSTS refers to posterior superior temporal sulcus; ACC refers to anterior cingulate cortex; IOG refers to inferior occipital gyrus; ACC refers to anterior cingulate gyrus; SPL refers to superior parietal lobule; TPJ refers to temporoparietal junction. Regions that share the same superscript are part of the same cluster.

Supplementary Figure 1. Most extreme frame displacements

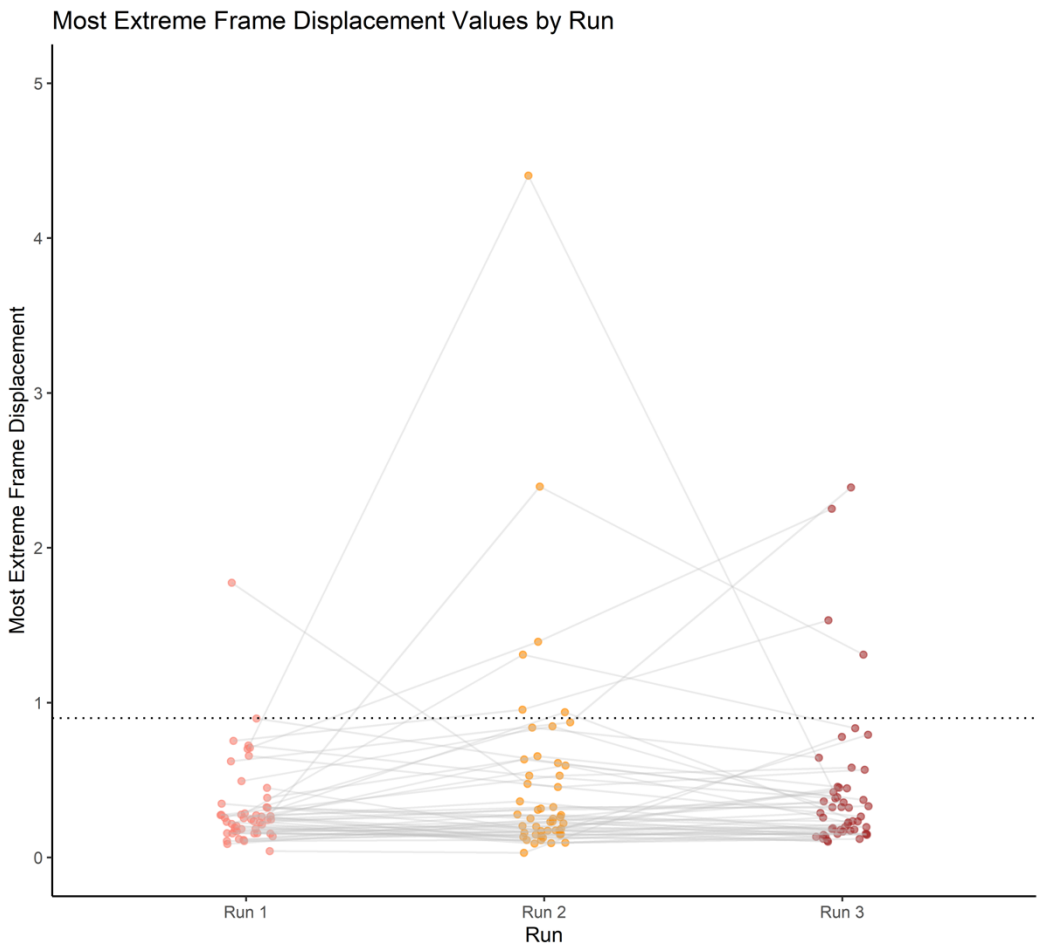

Note. Values are randomly jittered along the x-axis. Frame displacement values are in millimeter units. The dotted line corresponds to our frame displacement cutoff of 0.9.

Supplementary Figure 2. Ventral Striatum and Lateral Prefrontal Cortex Masks Used to Extract Univariate Activation Estimates

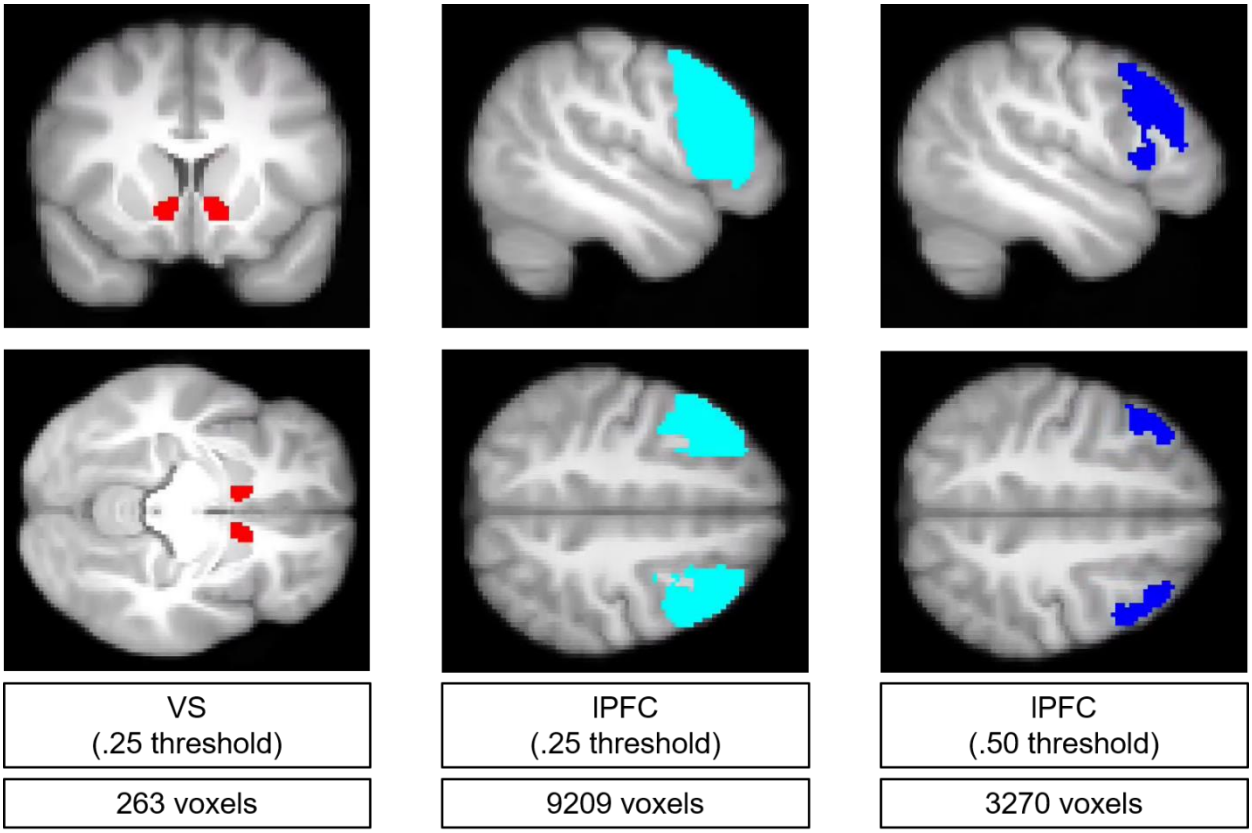

Note. NAcc refers to ventral striatum (NAcc); lPFC refers to lateral prefrontal cortex. Thresholds were applied to probabilities values from the Harvard-Oxford cortical and subcortical atlases. Masks are depicted in MNI standard space and projected onto an average of all subjects high resolution anatomical images.

Supplementary Figure 3. Results from the Go > Stop (top row) and Stop > Go (bottom row) contrasts.

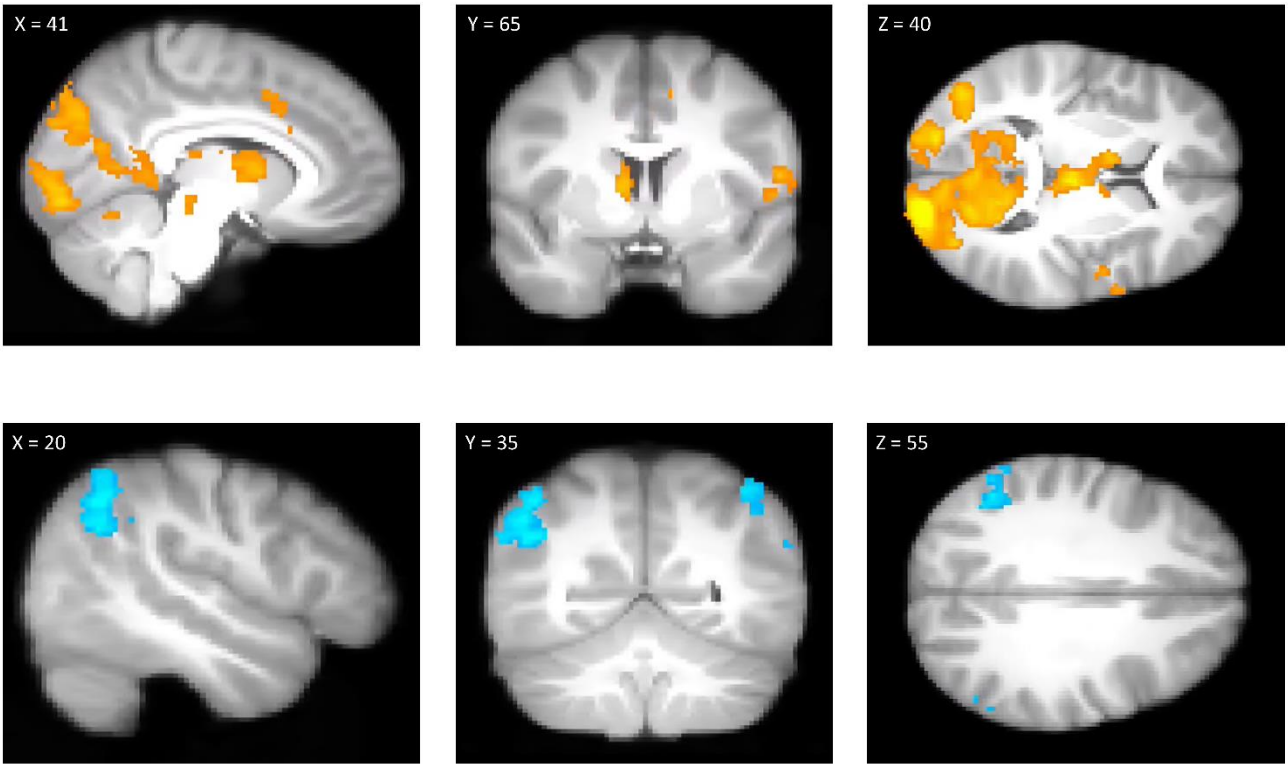

Note. XYZ refer to voxel coordinates in MNI standard space. Clusters rendered here were obtained using a cluster-defining-threshold of Z = 3.1, correct for multiple comparisons at $p < .05$ using Random Field Theory. Clusters are rendered on 'bg_image', FSL's average of all subjects' high resolution anatomical image.

Supplementary Figure 4. Multivariate signatures of Value (top row) and Cognitive Control (bottom row)

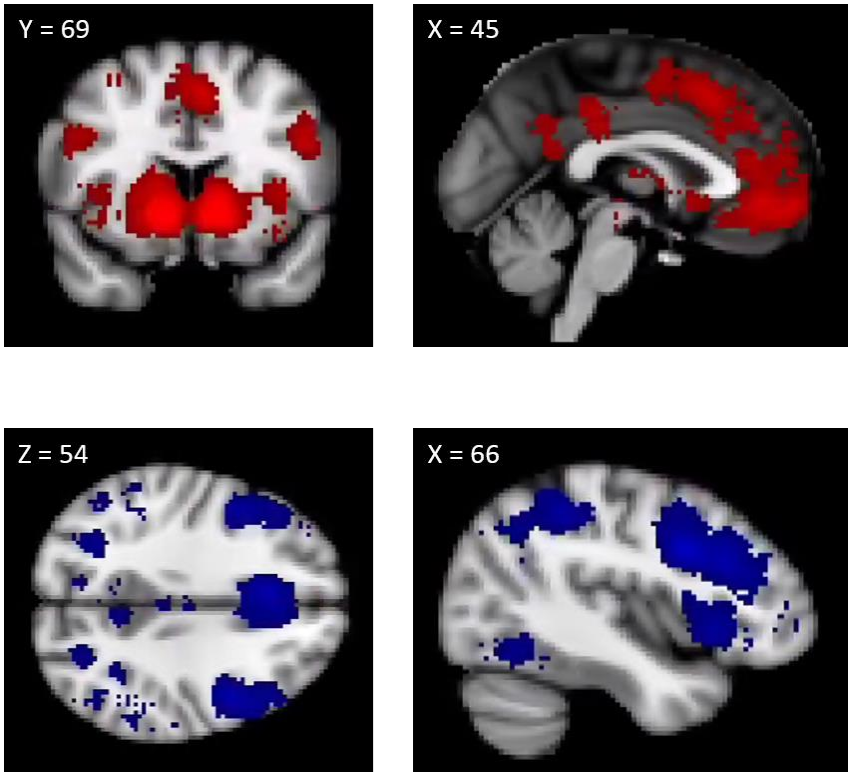

Note. Both signatures obtained from Neurosynth. Uniformity signatures are depicted here. Voxels weights differed between each mask (i.e., a hypothetical voxel could be included in both signatures, but its weight likely varied between signatures. This is important to note because these maps were used as multivariate signatures, which ultimate meant that the same brain regions included in both masks possessed a different multivariate signature.